Supplement of Nat. Hazards Earth Syst. Sci., 26, 5897–5907, 2026
https://doi.org/10.5194/nhess-26-5897-2026-supplement
© Author(s) 2026. CC BY 4.0 License.



Natural Hazards and Earth System Sciences
Open Access
EGU

Supplement of

Present and future trends of extreme short-term rainfall events in Germany, by downscaling convective environments of ERA5 and a CMIP6 ensemble

Gerd Bürger and Maik Heistermann

Correspondence to: Gerd Bürger (gerd.buerger@uni-potsdam.de)

The copyright of individual parts of the supplement might differ from the article licence.

S1 CatRaRE

Unlike Fig. 1 of the main text which displayed the CatRaRE events grouped into annual values, Fig. S1 shows the CatRaRE values with its original timestamp. Trend lines are estimated for the 99-, 99.9-, and 99.99-percentiles from quantile regression. None of the trends is significant (and remains so with the annual timestamp, not shown). The difference in significance, hence, results from the different estimation methods, that is, independent calculation of annual quantiles followed by trend estimation (Fig. 1) versus combined optimization of quantiles and trend (Fig. S1).

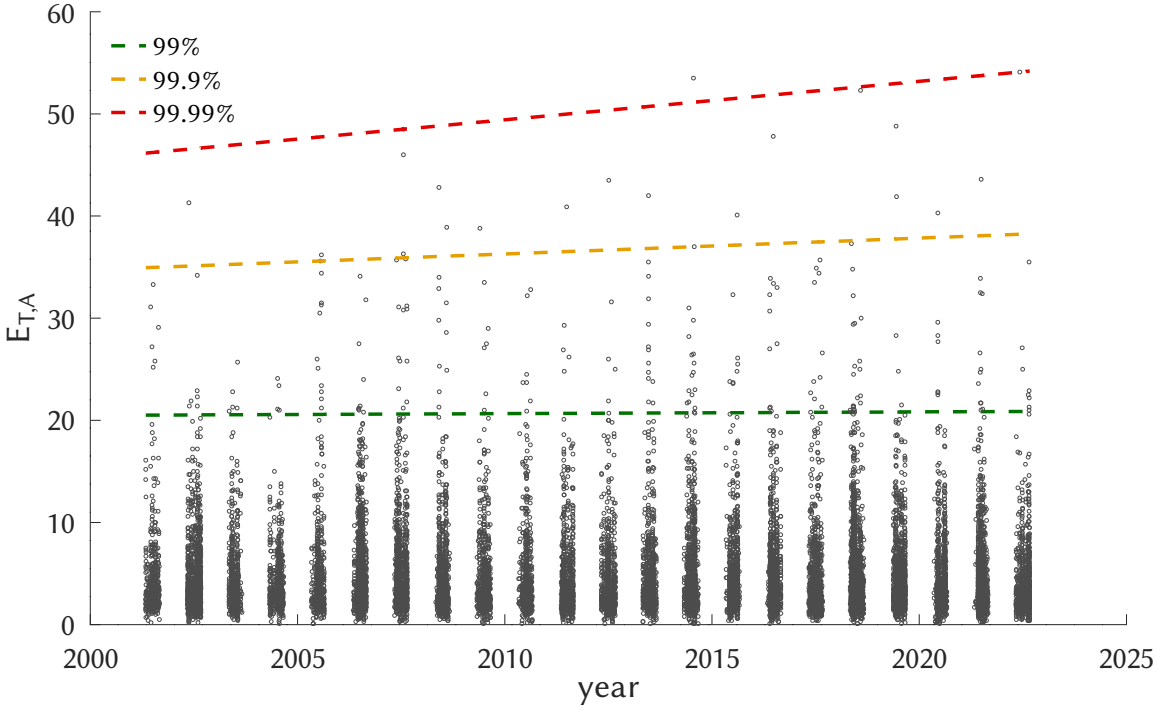


Figure S1. All CatRaRE events and corresponding trend lines for the 99-, 99.9-, and 99.99-percentiles, based on quantile regression. None of the centennial trends – 1.7, 15.5, and 37.6, resp. – is significant.

S2 Classification

S2.1 The 'shallow' classifiers

As in Bürger and Heistermann (2023, BH in the following), EOF reduction, based on North's rule of thumb, is performed on any of the atmospheric input fields prior to the application of a method; the number of retained EOFs is thus automatically derived from the respective eigenvalue spectrum.

S2.1.1 LASSO

We use the multinomial classifier *glm_multinomial* of McIlhagga (2016). To ensure probabilities that add up to 1 as outcome the softmax function is applied.

S2.1.2 TREE

As in BH we use a default setting of M5PrimeLab after EOF filtering; this implies to use a third of the input variables at random with replacement. By default, M5PrimeLab uses only linear predictor terms (cf. G. Jekabsons, author of M5PrimeLab).

S2.1.3 NLS

Here we use a somewhat non-standard approach: for each each single class a binary nonlinear least squares fit via Levenberg-Markwardt is performed, and the results aubsequently combined via the softmax function to obtain a full classification. The approach should be seen as merely heuristic.

S2.2 'Deep' classifiers

As explained in BH, the DL classifiers are used to frame the pattern classification problem of our study as one of image classification. The atmospheric pattern of *cape*, *cin*, and *cp* are re-interpreted now as the 3 color channels of a 2d image.

S3 ERA5 and CMIP6 driving the trained classifiers

As atmospheric drivers, the 2-dimensional fields of *cape* and *cin* are calculated from integrated atmospheric profiles of parcel buoyancy, cf. Eq. (1) and (2) of the manuscript. Buoyancy is obtained from the virtual temperature difference between parcel and environment, and is integrated between the LFC and the EL (*cape*) and EL and SFC (*cin*). The different levels as well as virtual temperature can be expressed as functions of atmospheric pressure, temperature, and specific humidity (Bolton, 1980), coded into the program getcape.F (https://github.com/pradeepfn/CM1/blob/master/src/getcape.F).

S3.1 ERA5

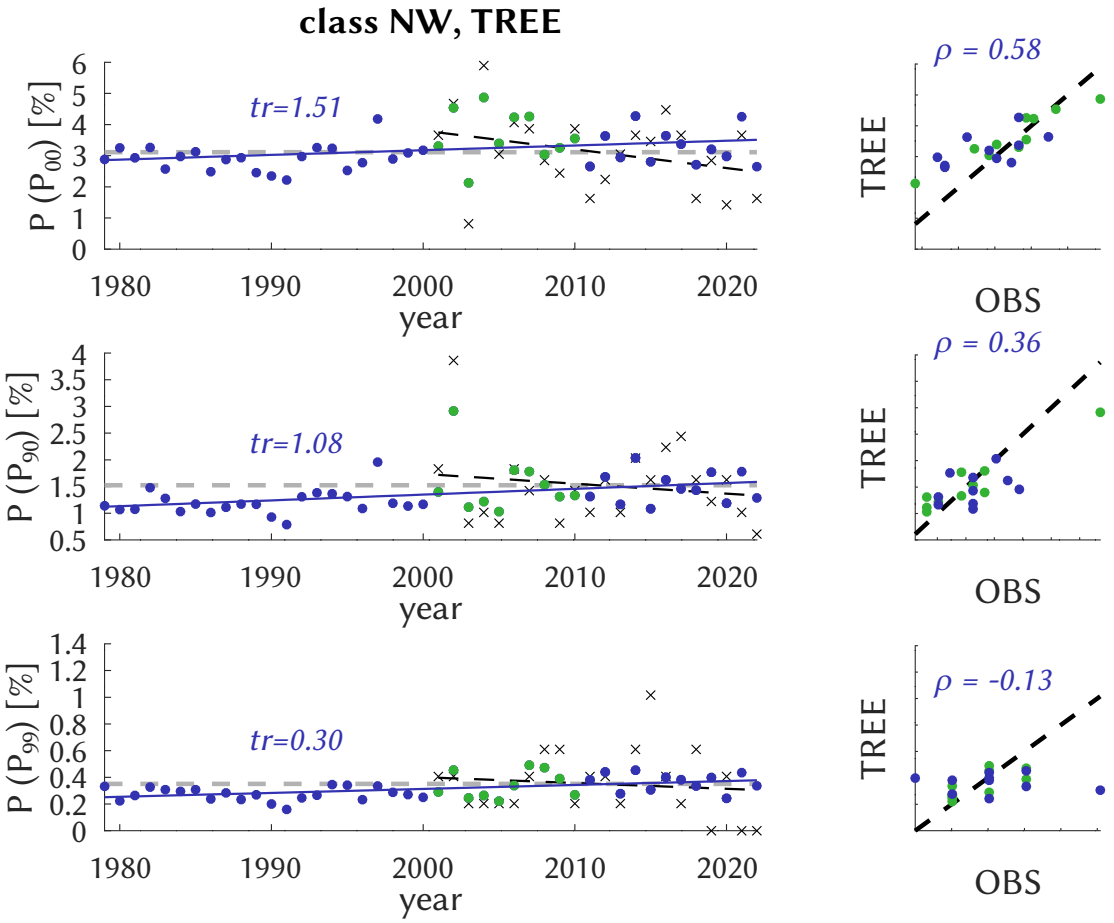


Figure S2. Like Fig. 6, for the NW class.

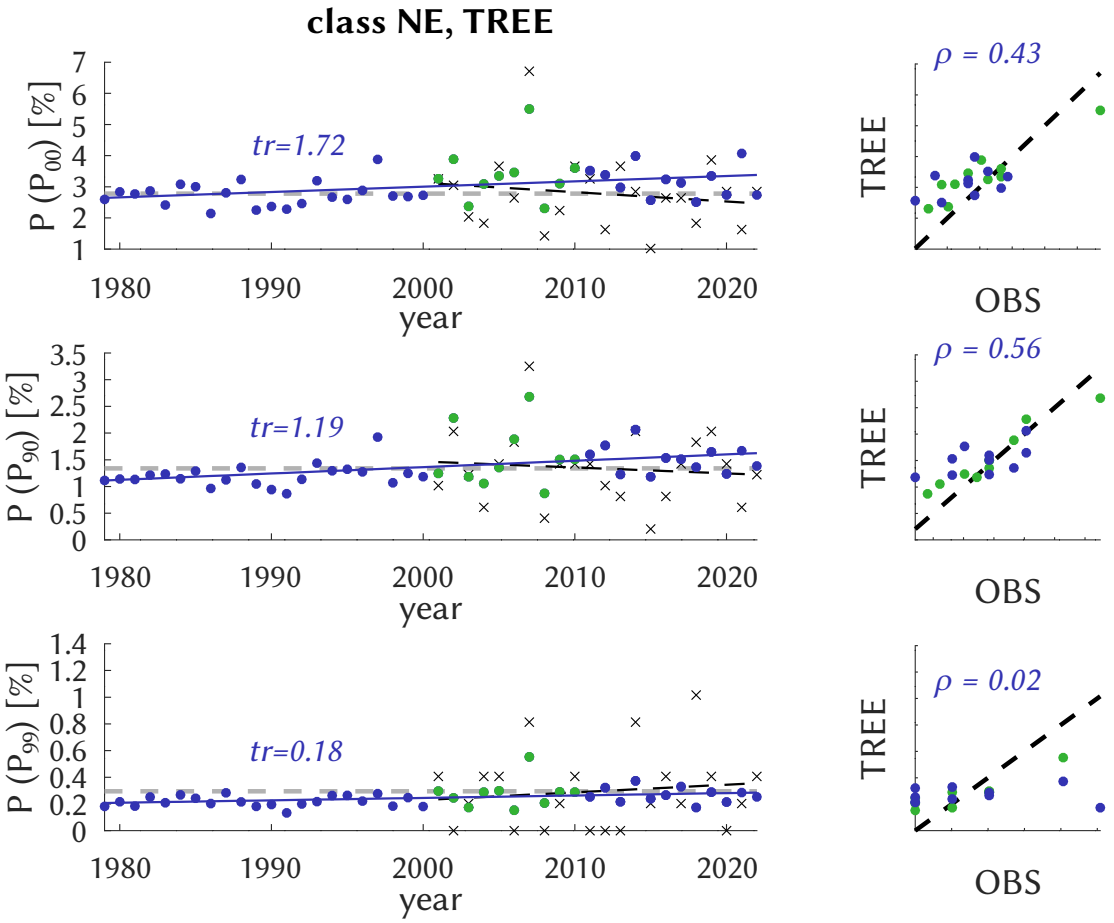


Figure S3. Like Fig. 6, for the NE class.

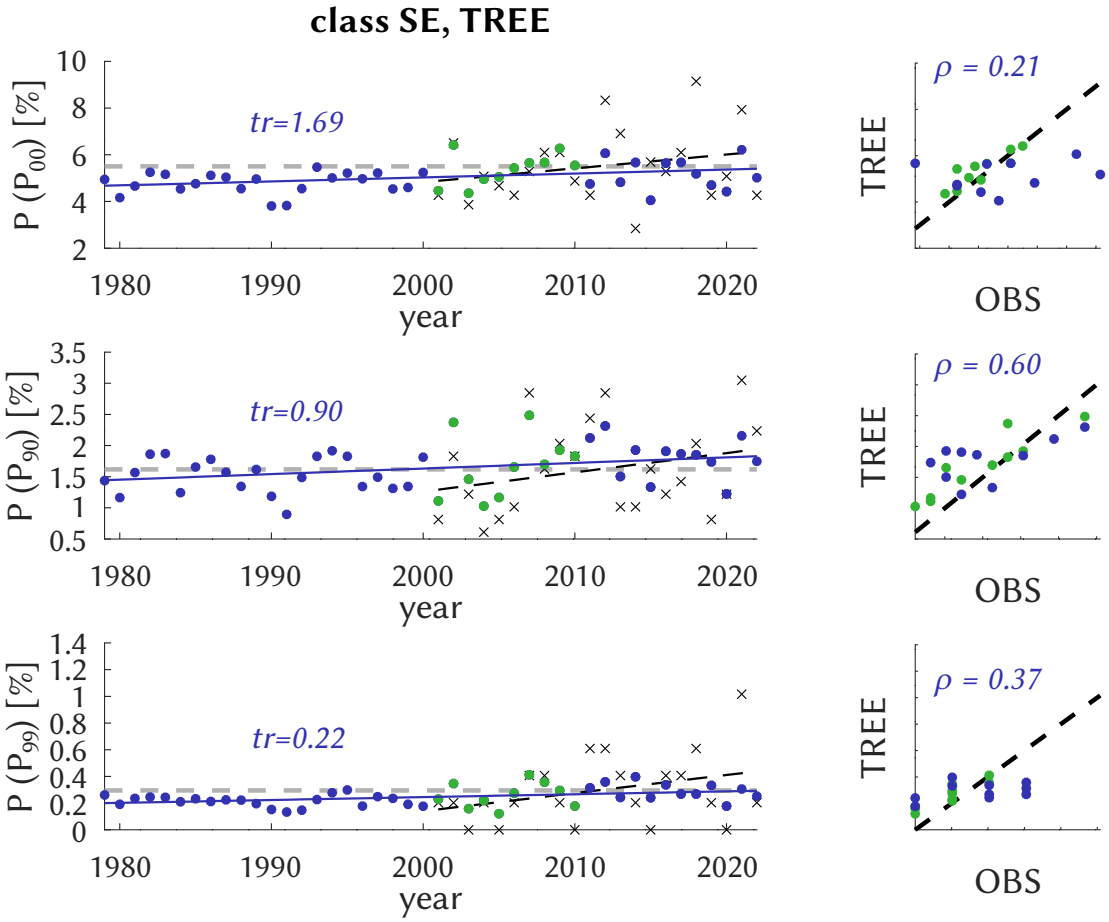


Figure S4. Like Fig. 6, for the SE class.

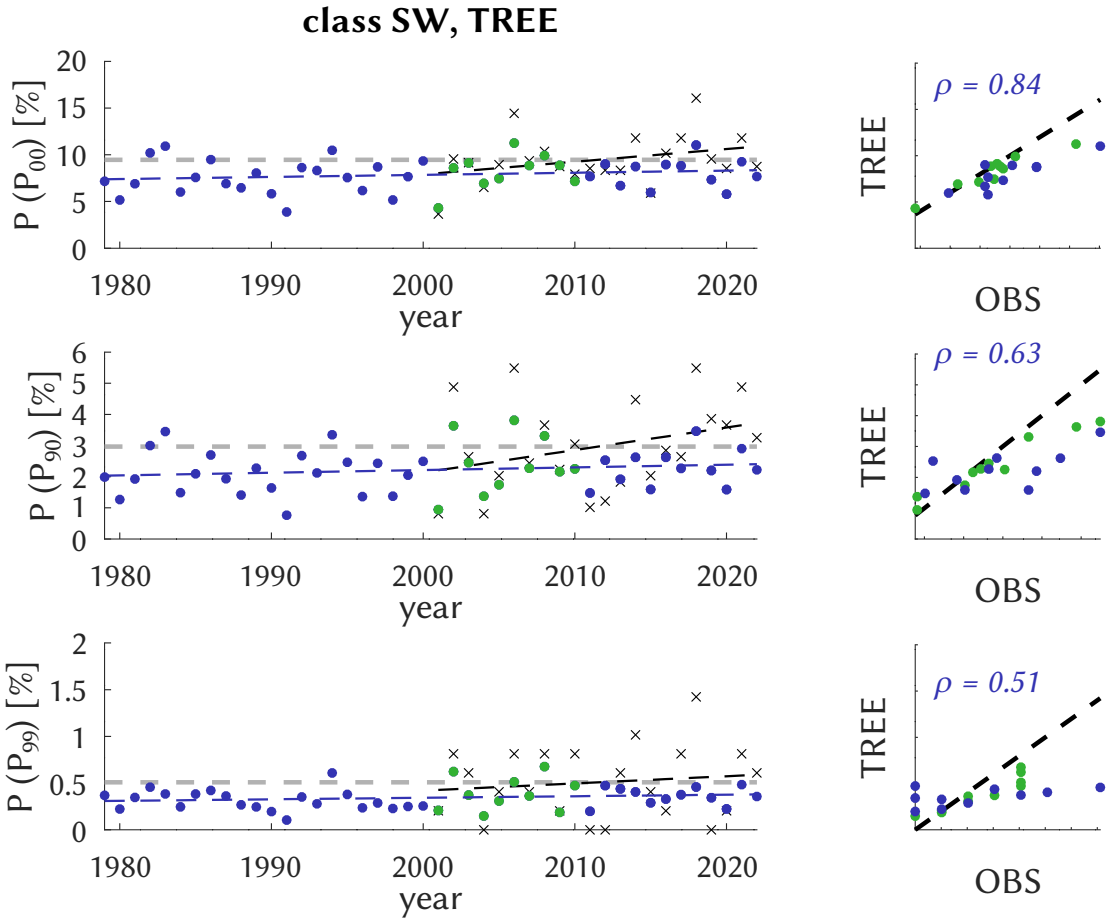


Figure S5. Like Fig. 6, for the SW class.

S3.2 CMIP6

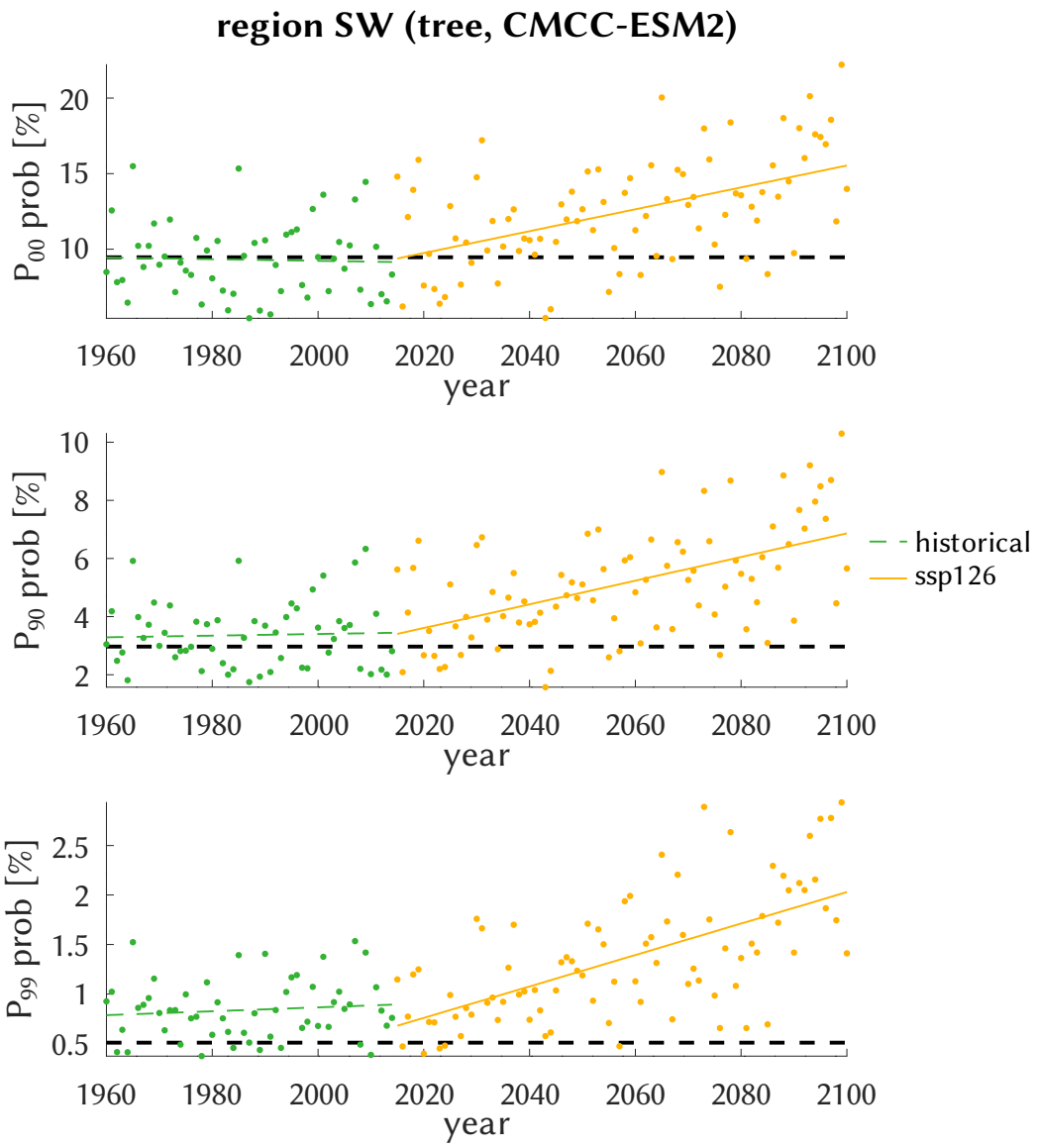


Figure S6. Like Fig. 7, based on the climate model CMCC-ESM2.

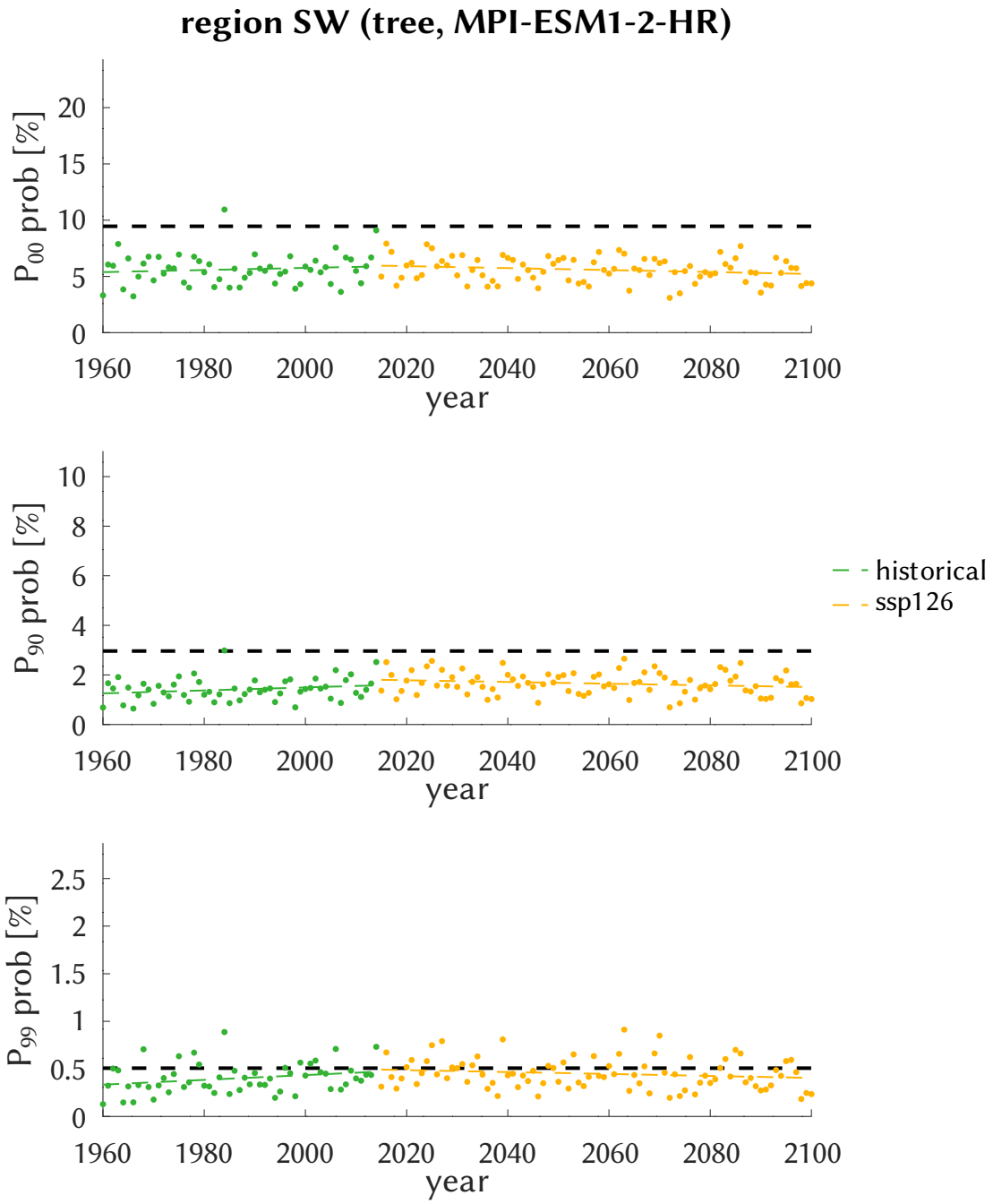


Figure S7. Like Fig. 7, for the r1 realization of MPI-ESM1-2-HR.

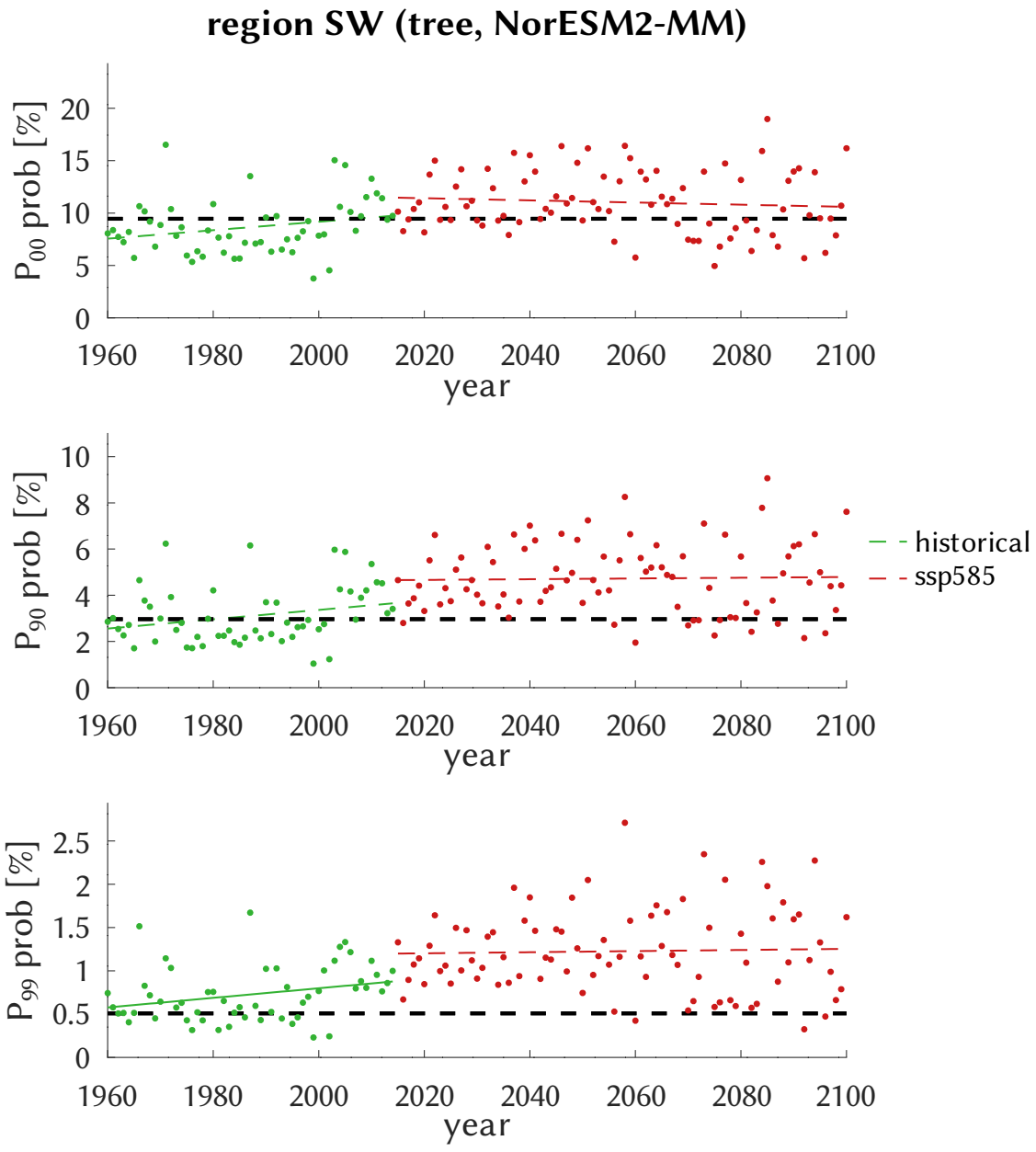


Figure S8. Like Fig. 7, for NorESM2-MM.

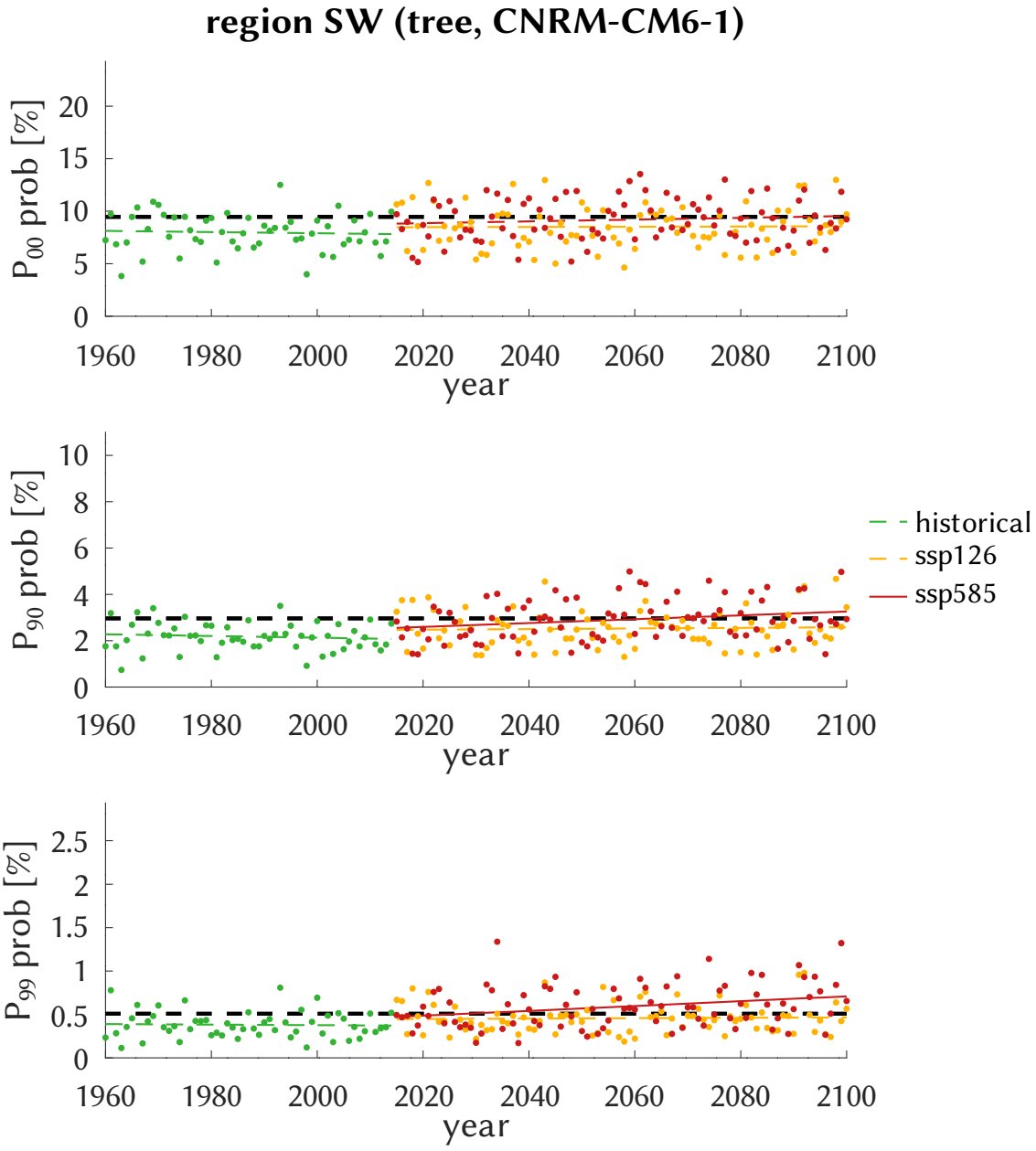


Figure S9. Like Fig. 7, for CNRM-CM6-1.

S3.3 Normalized drivers

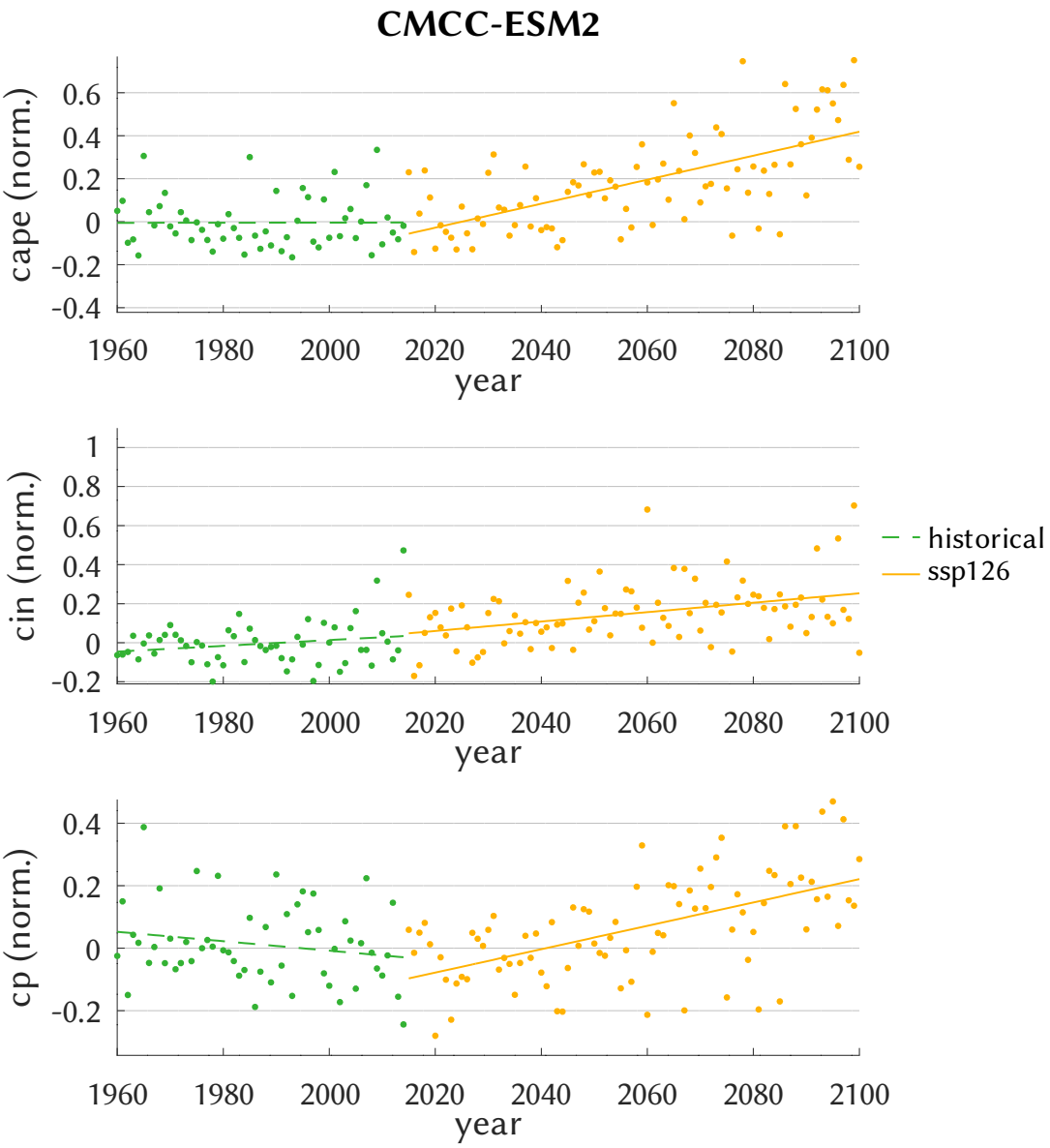


Figure S10. Like Fig. 8, for CMCC-ESM2.

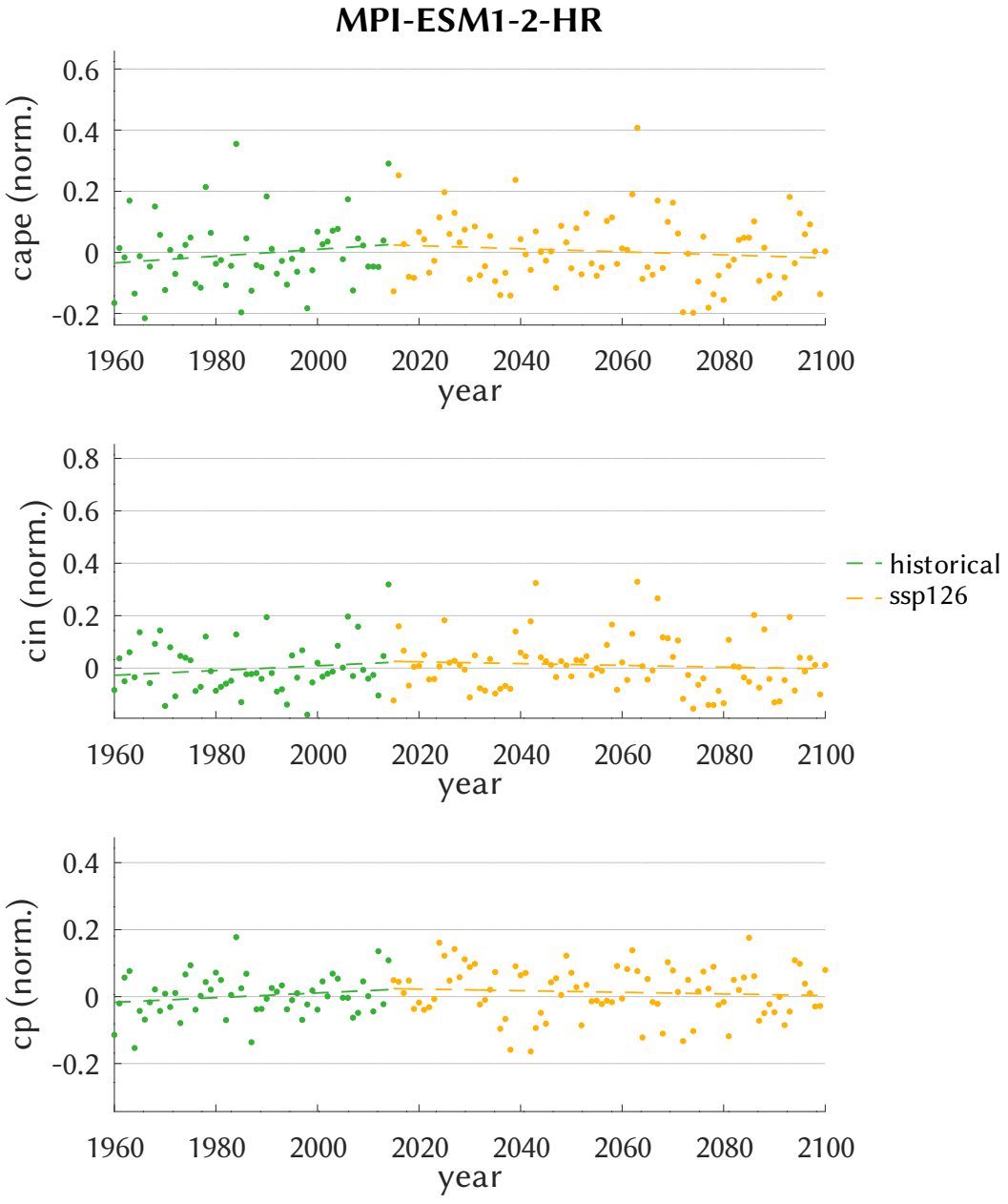


Figure S11. Like Fig. 8, for the r1 realization of MPI-ESM1-2-HR.

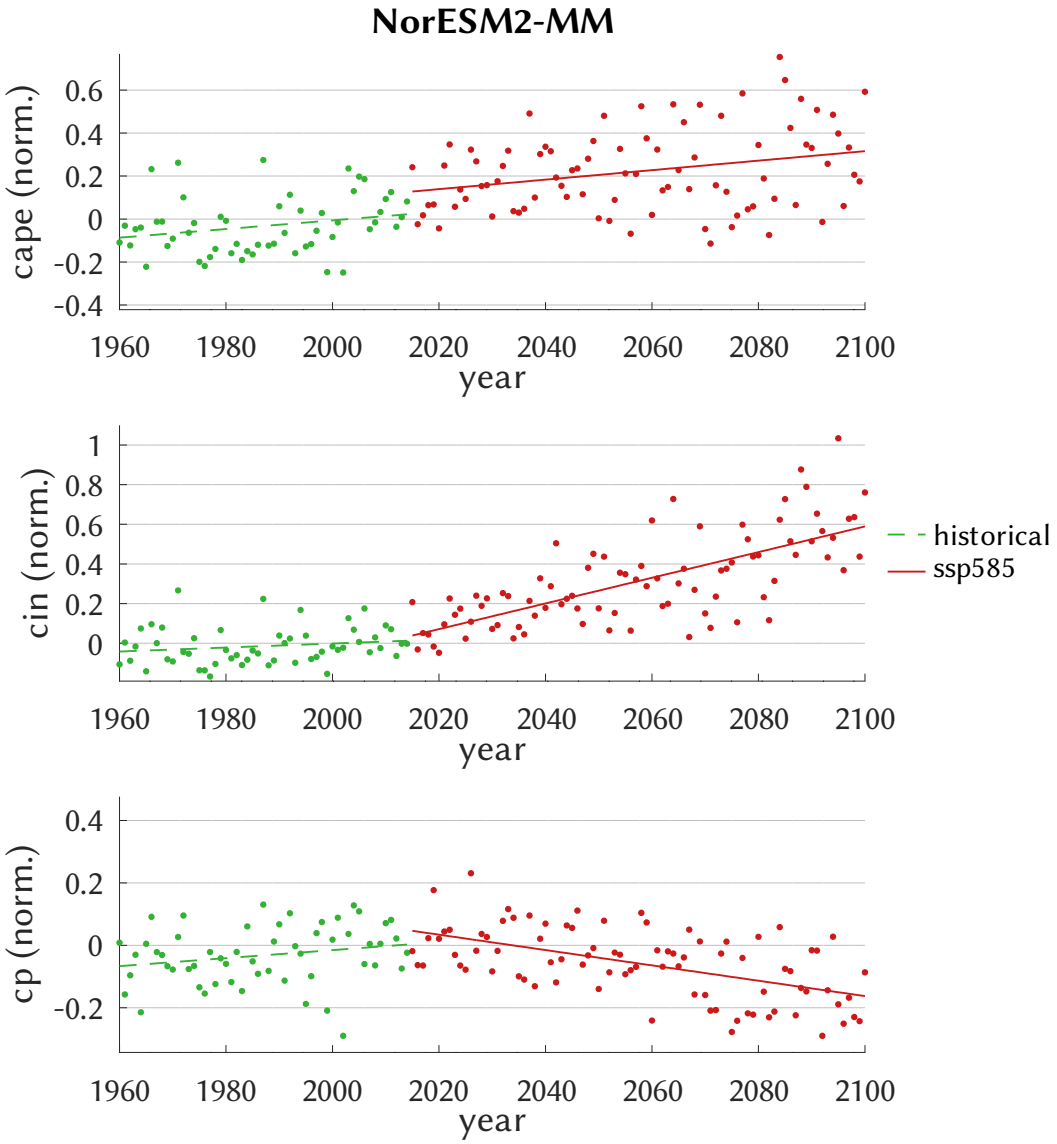


Figure S12. Like Fig. 8, for NorESM2-MM.

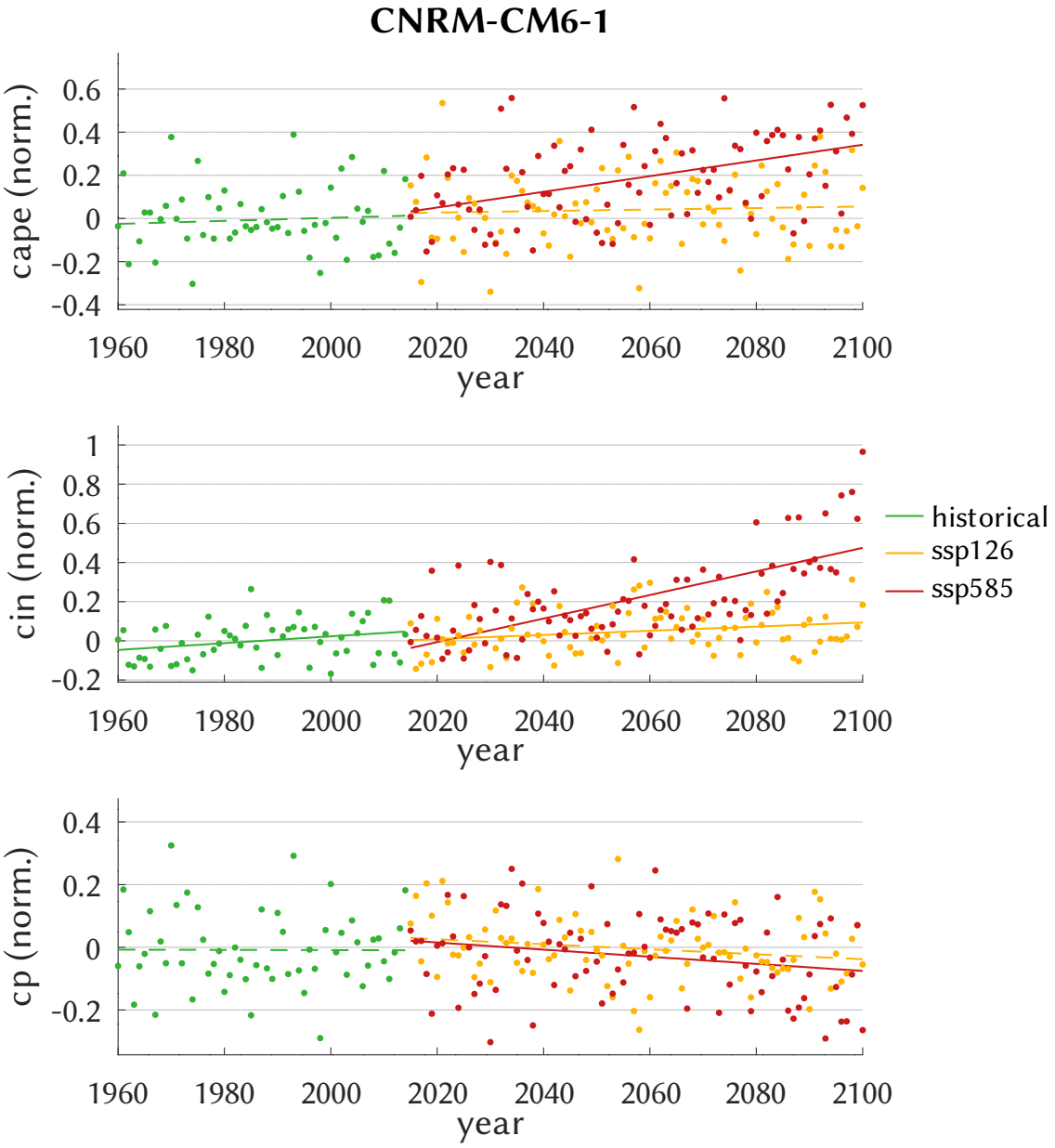


Figure S13. Like Fig. 8, for CNRM-CM6-1.

S4 Distribution and ANOVA of the simulated trends

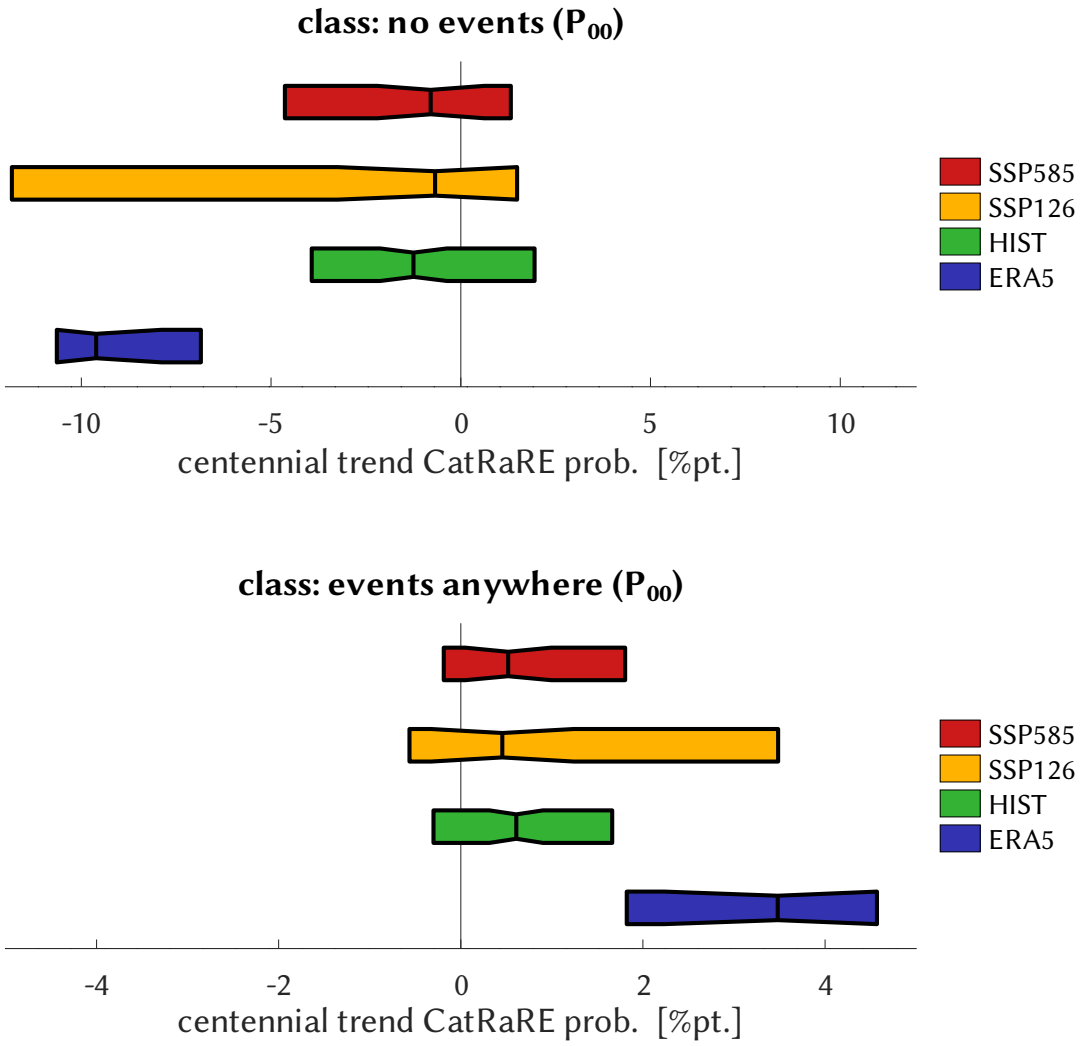


Figure S14. As Fig. 9, for the P_{00}-class.

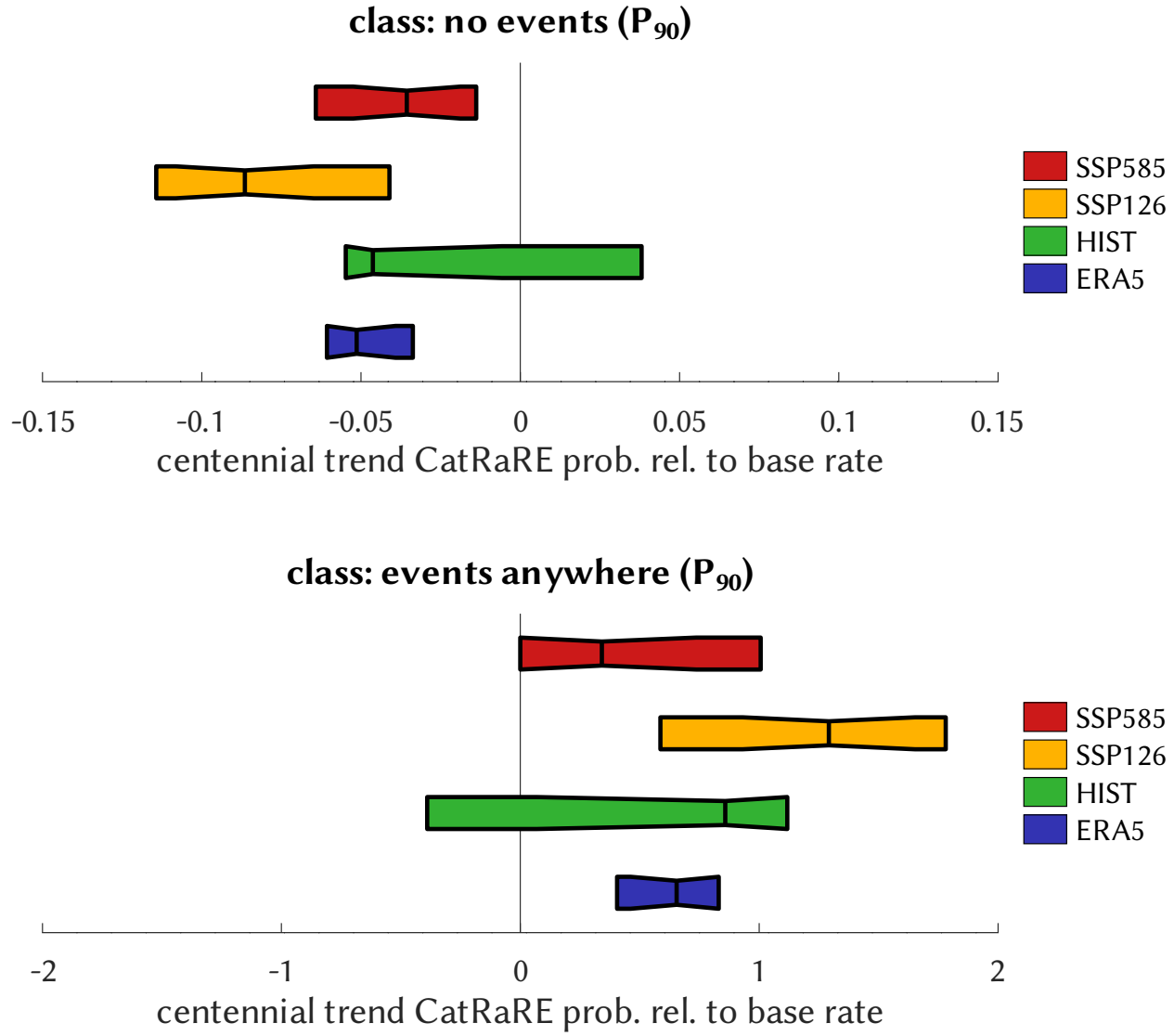


Figure S15. Similar to Fig. 9, confined to significant trends.

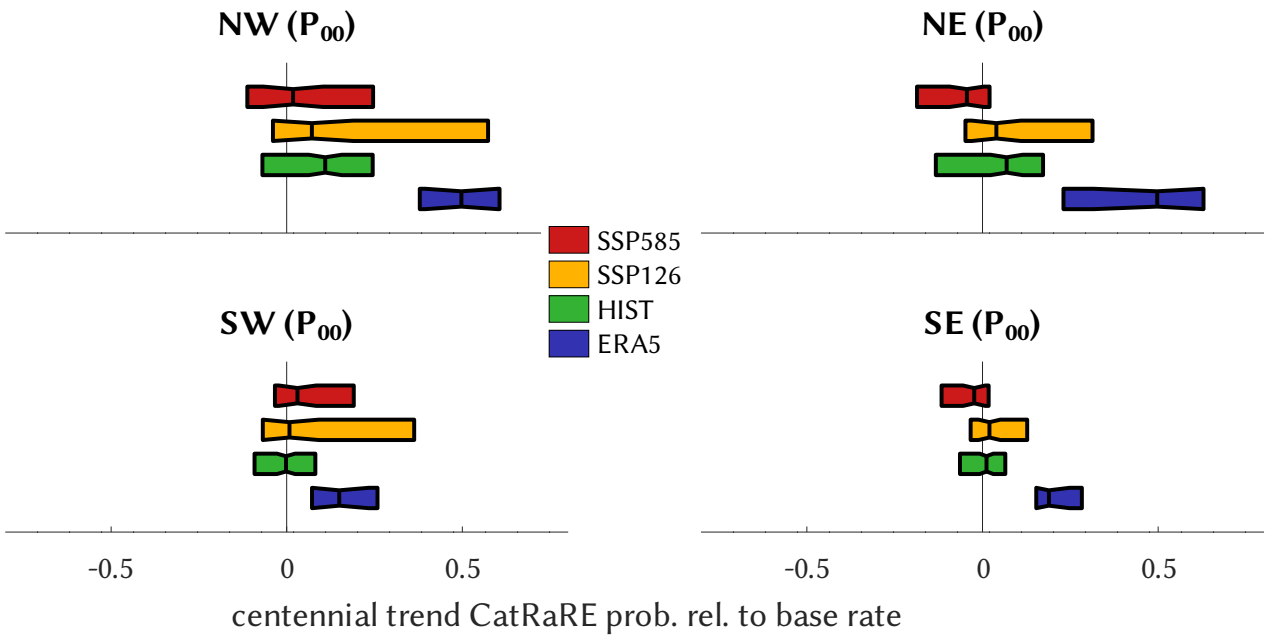


Figure S16. Like Fig. 10 for P_{00}.

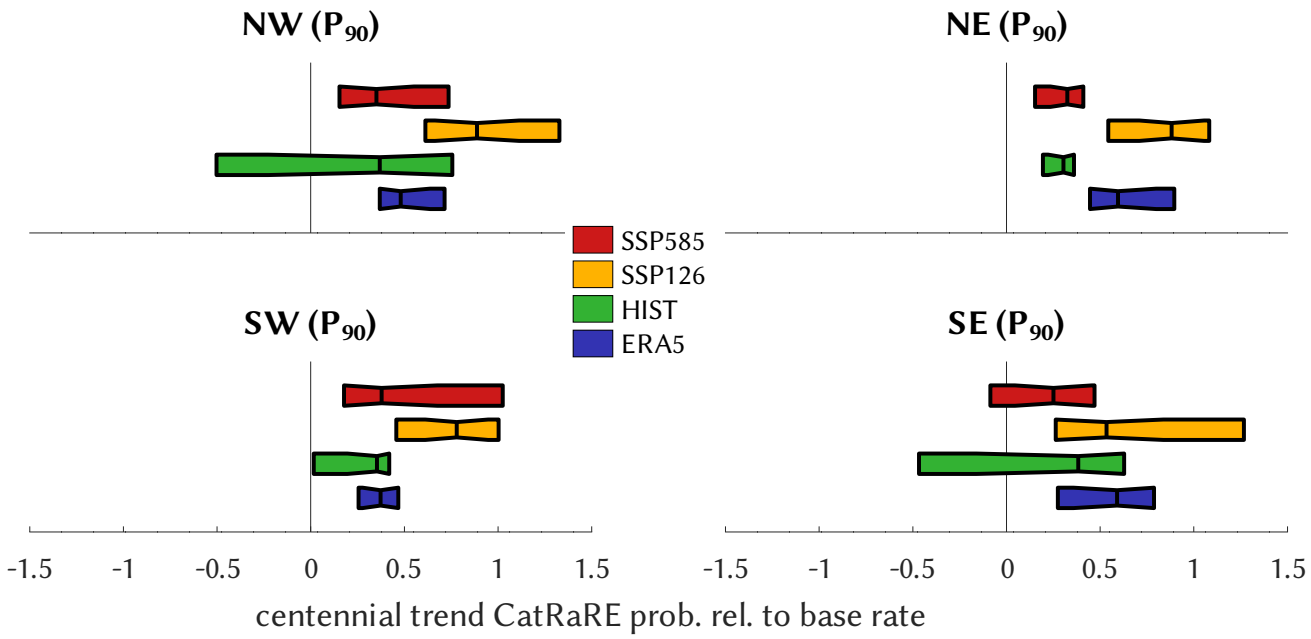


Figure S17. As Fig. 10, confined to significant trends.

S5 The relation between driver and CatRaRE trends

We finally check whether we can find any interrelationships between the trends of the driving atmospheric convective environments (*cape, cin, cp*) and the obtained CatRaRE-type events. Table 1 lists the corresponding correlations across all regions and severity classes. First of all, the strong positive correlation between *cape* and *cin* is apparent, demonstrating the simultaneous growth for the two antagonistic drivers for future convectivity (Chen et al., 2020; Lepore et al., 2021; Taszarek et al., 2021). The positive and negative correlations between *cp* on the one hand and *cape* and *cin*, respectively, on the other should hold per definitionem. It is unclear why it does not hold for CatRaRE which shows a positive, albeit negligible, correlation to *cin*.

Table S1. Correlations between centennial trends of convective environments and CatRaRE

	cape	***cin***	***cp***	**CatRaRE**
cape	*1*	*0.69*	*0.44*	*0.51*
cin		*1*	*-0.28*	*0.15*
cp			*1*	*0.50*
CatRaRE				*1*

References

Bolton, D.: The computation of equivalent potential temperature, Monthly weather review, 108, 1046–1053, 1980.

Bürger, G. and Heistermann, M.: Shallow and deep learning of extreme rainfall events from convective atmospheres, Natural Hazards and Earth System Sciences, 23, 3065–3077, https://doi.org/10.5194/nhess-23-3065-2023, 2023.

Chen, J., Dai, A., Zhang, Y., and Rasmussen, K. L.: Changes in Convective Available Potential Energy and Convective Inhibition under Global Warming, Journal of Climate, 33, 2025–2050, https://doi.org/10.1175/JCLI-D-19-0461.1, 2020.

Lepore, C., Abernathey, R., Henderson, N., Allen, J. T., and Tippett, M. K.: Future Global Convective Environments in CMIP6 Models, Earth's Future, 9, e2021EF002277, https://doi.org/10.1029/2021EF002277, 2021.

McIlhagga, W.: penalized: A MATLAB Toolbox for Fitting Generalized Linear Models with Penalties, Journal of Statistical Software, 72, 1–21, https://doi.org/10.18637/jss.v072.i06, 2016.

Taszarek, M., Allen, J. T., Marchio, M., and Brooks, H. E.: Global climatology and trends in convective environments from ERA5 and rawinsonde data, npj Clim Atmos Sci, 4, 1–11, https://doi.org/10.1038/s41612-021-00190-x, 2021.